Dynamic polarization of deuterium nuclei in completely deuterated ethanediol and propanediol

N. C. Borisov, É. I. Bunyatova, M. Yu. Liburg, V. N. Matafonov, A. B. Neganov, and Yu. A. Usov

Joint Institute for Nuclear Research, Dubna

(Submitted 6 June 1984)
Zh. Eksp. Teor. Fiz. **87**, 2234–2243 (December 1984)

A polarization of around 0.40 has been achieved for the deuterium nuclei in completely deuterated ethanediol and propanediol-1,2 containing a synthesized-in pentavalent chromium complex. The spin-lattice relaxation time in a magnetic field of 0.32 T and at a temperature $T = 0.054$ K is 10–15 h, which suggests that it should be possible to use these materials in "frozen" targets. Our studies permit the conclusion that the main mechanism for the dynamic orientation of deuterium nuclei in these materials is dynamic cooling. We report the characteristics of these materials and briefly describe the experimental apparatus and the equipment and procedures for processing the magnetic resonance spectra of the deuterium nuclei.

Targets containing polarized hydrogen and deuterium nuclei are widely used in many areas of high- and intermediate-energy physics. Among the wide variety of target types, which are chosen to suit the specifics of the experiment, the so-called "frozen" targets enjoy a special status.[1] In these the polarization of the nuclei remains practically unchanged over times of the order of a hundred hours even in a relatively weak magnetic field ($\leqslant 0.5$ T). Because of this the magnets producing the "sustaining" field can be designed in such a way that the scattered particles can be detected over a much larger region of solid angles.

Deuterated propanediol-1,2 ($C_3D_8O_2$) and ethandediol ($C_2D_6O_2$), which together are called diols, are used to prepare targets containing polarized deuterons. The paramagnetic centers necessary for the dynamic method of polarizing the nuclei are introduced into these materials by dissolving stable paramagnetic complexes of pentavalent chromium in them.[2,3] It has been shown,[4] however, that the HMBA-Cr(V) complex, for example, is unstable; it reacts with the solvent to form various paramagnetic complexes. The presence of these new complexes can sharply reduce the spin-lattice relaxation time, i.e., the material can become unsuitable for use as a frozen polarized target. Until recently it was believed that the stable complex Cr(V) cannot by synthesized in completely deuterated diols. However, it was shown in Ref. 5 for the case of ethanediol that this complex can in fact be synthesized at the necessary concentration of paramagnetic centers for the dynamic method of polarization. This opens up the possibility of using these materials for frozen polarized targets. In this paper we investigate the suitability of these materials for such a use.

SPIN TEMPERATURE

The concept of spin temperature[6,7] implies that a solid can support conditions such that it is possible to isolate a separate thermodynamic subsystem associated with the spin degrees of freedom. In our case this comprises the nucler spin systems (NSS), which are different for nuclei of different kinds, and the electronic spin system (ESS), which is associated with the spin degrees of freedom of the paramagnetic centers. Within each of the systems over a time $\sim\tau_2$—the internal (spin-spin) relaxation time—a statistical equilibrium is established, with a characteristic spin temperature which over a time $\sim\tau_1$—the spin-lattice relaxation time—becomes equal to the temperature of the thermostatic bath. The necessary relationship of the relaxation times, $\tau_1 \gg \tau_2$, is always satisfied for a solid at low temperatures. In addition, in frozen diols $\tau_1 \approx 0.1$ sec over a wide range of low temperatures for the ESS, whereas for the NSS the spin-lattice relaxation time ranges from 1 to 10^2 h at temperatures from 0.3 to 0.02 K.[8–10]

Subjecting the material to a microwave electromagnetic field at a frequency close to an electron paramagnetic resonance (EPR) initiates cyclic processes in the ESS which lower the spin temperature in the NSS. The coupling that arises here between the ESS and the NSS (customarily called the induced contact) establishes a single spin temperature in all the NSS. This is one of the outstanding features of the so-called dynamic cooling effect.[8,11] Another possible method of lowering the temperature of the NSS uses a microwave pump to induce transitions between the magnetic sublevels of the system consisting of the nuclear spin and the electron spin, which are coupled by the dipole-dipole interaction.[12] Here the pumping does not affect the spins of the other NSS; this is the so-called "differential solid effect."[8]

The spin temperature T_s is related to the polarization $P(1/2)$ or $P(1)$ (the nuclear spin is given in the parentheses) by the expression for the Brillouin function[12]

$$P(^1/_2) = \operatorname{th}(\nu_H h/2kT_S), \tag{1}$$

$$P(1) = \frac{4\operatorname{th}(\nu_D h/2kT_S)}{3+\operatorname{th}^2(\nu_D h/2kT_S)}, \tag{2}$$

where ν_H and ν_D are the nuclear-magnetic-resonance (NMR) frequencies of the corresponding nuclei, k is the Boltzmann constant, and h is Planck's constant.

Polarization measurements usually involve a processing of NMR spectra. The most widely used method for hydrogen nuclei (protons) is based on the linear relationship between the integrated intensity of the NMR spectrum and

0038-5646/84/121291-06$04.00

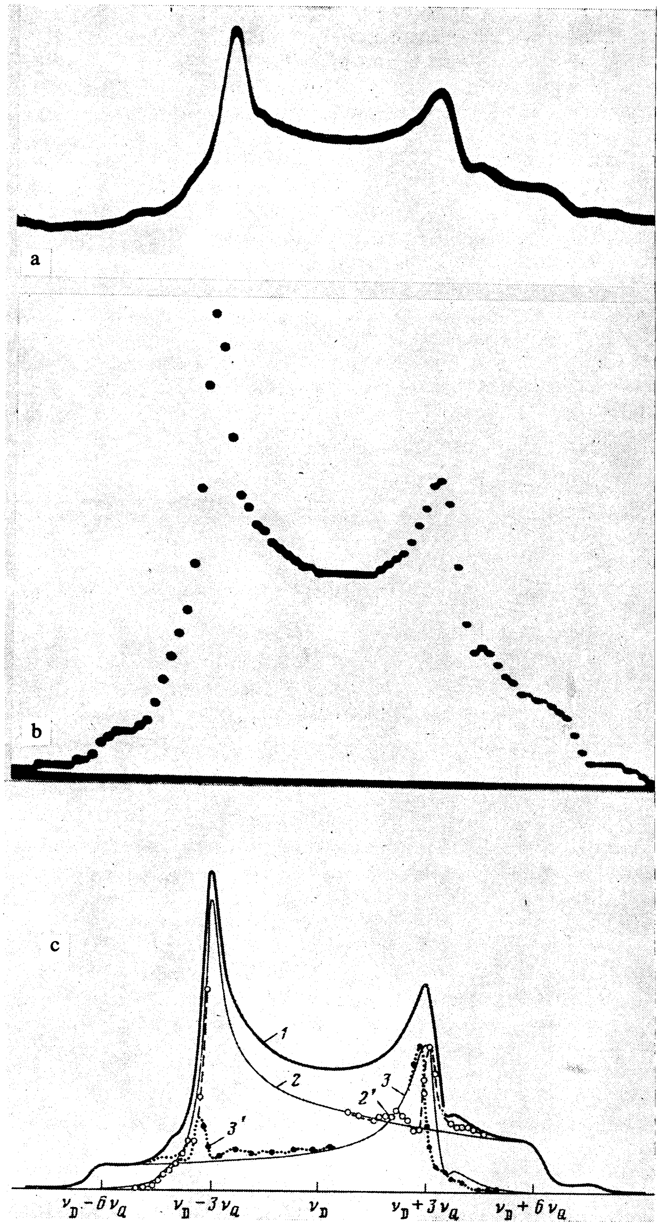

FIG. 1. Deuteron magnetic resonance spectrum (maximum negative polarization): a) DMR signal on oscilloscope; b) continuous DMR spectrum after analog-to-digital conversion, output to a graphic display; c) processing of the DMR spectrum. The total shape function of the spectrum (curve 1) is a superposition of the two functions (curves 2 and 3) corresponding to the transitions $m = -1 \to m = 0$ and $m = 0 \to m = 1$. The dashed curves show the regions where the functions Ψ_i and φ_i and also Ψ_{ai} and φ_{ai} do not coincide (see text proper for more details).

the polarization. When the NSS is in a state of thermal equilibrium with the lattice, the polarization is calculated using formulas (1) or (2) with T_S set equal to the temperature of the bath. However, to record equilibrium spectra at a temperature of 0.5 K in a magnetic field of 2–3 T is a rather complicated problem even for protons because of the low level of the useful signal relative to the level of noise and interference.[8] For deuterium nuclei the signal-to-noise ratio is almost a hundred times worse.[8] Therefore, the polarization of deuterium is more offten measured by another method—from the shape of the deuteron magnetic resonance (DMR) signal. The character of the DMR spectrum is affected substantially by the interaction of the deuteron quadrupole moment eQ with the inhomogeneous electric field within the molecule. For the case of an axially symmetric electric-field-gradient tensor with a value eQ along the principle axis of the tensor (the z axis is directed along the external magnetic field), in the first order of perturbation theory one can obtain the following expression for the mth magnetic energy level ($m = \langle I_z \rangle$) of the deuteron ($I = 1$) (Refs. 6 and 8):

$$E_m = -\nu_D h m + {}^1/_8 e^2 qQ (3\cos^2\vartheta - 1)[3m^2 - I(I+1)]. \qquad (3)$$

The first term describes the Zeeman splitting: ν_D is the central frequency of the DMR spectrum. The contribution from the quadrupole interaction depends on the angle ϑ between the z axis and the principal axis of the electric-field-gradient tensor; the latter axis is assumed to lie in the direction of the C–D or O–D bonds.[8] In frozen diols, which are amorphous materials, all orientations of the C–D and O–D bonds are equally probable. The shifts of the Zeeman-split energy levels are multiples of $\nu_Q = e^2qQ/8h$, and therefore the shape function of the DMR spectrum (Fig. 1) is a superposition of two curves, 2 and 3, corresponding to the transitions $m = -1 \to m = 0$ and $m = 0 \to m = +1$. The ratio of the areas under these curves is commonly called the asymmetry. Denoting by n_+, n_-, and n_0 the relative populations of the levels with $m = 1, -1$, and 0, respectively, we have the following expression for the asymmetry:

$$R = (n_+ - n_0)/(n_0 - n_-).$$

Since the magnetic energy levels are populated in accordance with the Boltzmann distribution, we have

$$R = n_+/n_0 = n_0/n_-.$$

For the polarization P_D and alignment A we have by definition[12]

$$P_D = n_+ - n_-, \quad A = 1 - 3n_0,$$

or

$$P_D = \frac{R^2-1}{R^2+R+1}, \quad A = \frac{(R-1)^2}{R^2+R+1}. \qquad (4)$$

The polarization and alignment can be calculated from the experimental value of R with the aid of formulas (4), which were derived with allowance for the existence of a spin temperature in the NSS associated with the deuterons in diols at low lattice temperatures.[8]

THE SAMPLES

The investigated materials consisted of a complex compound of pentavalent chromium Cr(V) in deuterated dioles—ethanediole, general formula $C_2D_6O_2$, and propanediol-1,2, general formula $C_3D_8O_2$. The dynamic polarization of deuterons was studied in three samples (see Table I). To increase the surface area the samples were made into frozen spheres 2 mm in diameter.

Sample No. 1 was a Cr(V) complex in deuterated ethanediol, containing 98.5 at. % deuterium in a substitutional position. The synthesis of the complex is described in Ref. 5. The electron-paramagnetic resonance (EPR) spectra of the complex at room temperature and liquid-nitrogen tempera-

TABLE I.

Sample no.	Material	D content, wt. %		Relaxation			Maximum polarization P_D
				B, T	T, mK	τ_1, h	
1	Ethanediol $(CD_2OD)_2$	17,6	$(5\pm1)\cdot10^{19}$	0.32	54	10	$-(0.42\pm0.02)$
					54	15	$+(0.42\pm0.02)$
2	Ethanediol $(CD_2OD)_2$	17,6	$1\cdot10^{19}$	2,08	800	4	0,10
3	Propanediol -1,2 $C_3D_6(OD)_2$	19,0	$(6\pm1)\cdot10^{19}$	0,32	80	1	$+(0.38\pm0.02)$ $-(0.41\pm0.02)$

ture we recorded on a Varian E-12 spectrometer. At room temperature the linewidth was $\Delta H = 4.5\cdot10^{-4}$ T, and the g factor evaluated from the position of the line relative to that of the iminoxyl radical 2,2,6,6-tetramethylpiperidine-1-oxyl (with $g = 2.0064$), was 1.979. The concentration (per cm^3) of paramagnetic centers (p.c.) was $(5 \pm 1)\cdot10^{19}$ p.c./cm^3. The concentration was measured by comparing the parameter $h(\Delta H)^2$ of the sample with that of a reference material—dibenzolchromium iodide in $C_2D_6O_2$.

Sample No. 2 was also a Cr(V) complex in $C_2D_6O_2$. The sample was prepared by diluting the original sample No. 1, with a concentration of $(5 \pm 1)\cdot10^{19}$ p.c./cm^3 (taken to be unity), by deuterated ethanediol in a ratio of 1:6.

In the present paper we have carried out the first successful synthesis of a Cr(V) complex in completely deuterated propandiol-1,2 ($C_3D_8O_2$), which follows ethanediol alcohol in the homoloogous series of diols. The Cr(V) complex was obtained in a reduction reaction of $K_2Cr_2O_7$ in $C_3D_8O_2$. Deuterated propanediol-1,2 containing 98.3 at. % deuterium in a substitutional position was prepared at our request by the State Institute of Applied Chemistry in Leningrad. We studied the reaction responsible for the formation of the Cr(V) complex in completely deuterated propanediol in order to determine the reaction conditions (such as the temperature, reaction time, and initial bichromate concentration). As a result we were able find the optimum conditions and thus to obtain a complex (sample No. 3) with a concentration of $(6 \pm 1)\cdot10^{19}$ p.c./cm^3 (measured by an EPR method). The EPR linewidth of the complex at room temperature was $\Delta H = 5\cdot10^{-4}$T.

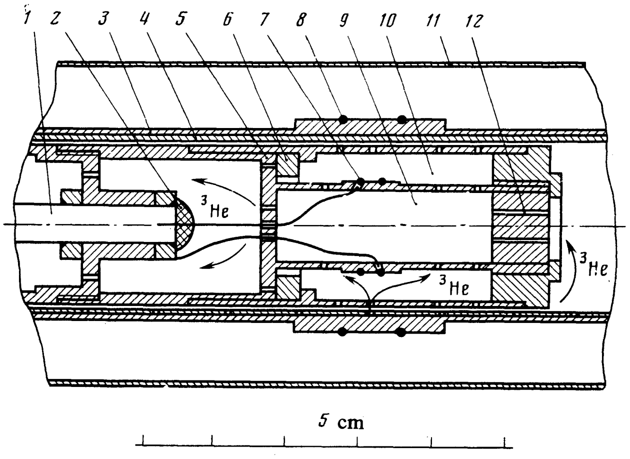

FIG. 2. Dissolution chamber with ampoule for samples: 1) cable of rf coil; 2) sealed electrical lead; 3,4) Teflon casing of dissolution chamber; 5) support member; 6) ring flange; 7) inner rf coil (the main coil in these experiments); 8) outer coil; 9) volume filled with sample; 10) space for heater; 11) microwave resonator; 12) stopper.

APPARATUS

The experiments were done on a PPZM-200 apparatus—a proton frozen target with a longitudinal dimension (along the particle beam) of 200 mm.[9] The main part of the apparatus is a horizontal He^3–He^4 dissolution cryostat. The target material, made into spheres 2 mm in diameter, was poured into a special container and inserted along the central channel of the cryostat into the dissollution chamber, at liquid-nitrogen temperature. The dissolution chamber was then hermetically sealed, and the central channel was evacuated. In the dissolution regime, precooled He^3 entered the dissolution chamber, which was filled with a solution of He^3 in He^4, and was thence transported by the osmotic pressure drop into an evaporator and was subsequently pumped out by an external pump system.

For the present experiments the working container was replaced by a special Teflon ampoule inserted into the dissolution chamber (Fig. 2). The induction coil consisted of five turns of silver-plated copper wire wound on a core which doubled as the sample container. The coaxial cable along the central channel consisted of an unperforated stainless steel tube (with a diameter of 5 mm and a wall thickness of 0.15 mm) and a bronze core (0.3 mm in diameter), held on the axis of the tube by Teflon spacers. Apertures in the walls of the ampoule and container admitted He^3 into the volume containing the investigated material; the He^3 was made to enter from below in order to give the best conditions for dissolution cooling) and to eliminate the possibility of a temperature drop along the sample.[10] The temperature of the sample was determined from the resistance of Speer-100 and Speer-200 carbon resistors, which were calibrated in a separate experiment on the basis of the NMR signals from the protons in a sample with a short spin-lattice relaxation time. A wire heater in space 10 (see Fig. 2) could release a fixed amount of heat energy in the dissolution bath to enable estimates of the microwave power dissipated in the dissolution bath during the pumping. In the absence of microwave power input the remaining energy evolution is due mainly to the influx of heat along the coaxial cable. The total parastic influx of heat into the dissolution chamber amounted to about $2\cdot10^{-4}$ W, raising the minimum temperature of the sample to 54 mK.

The NMR spectra were recorded with a Q meter in which the amplitude of the signals at the output is proportional to the resonance absorption of rf energy in the coil of an LC circuit.[12] The NMR spectrum is obtained by a sweeping of the frequency of the power oscillator over the 13.420 to 13.820 MHz range in a nearly linear manner.

A parallel LC circuit was formed by the induction coil and the capacitance of the cable, together with an additional parallel capacitance connected at the input of the Q meter. The cable was constructed in such a way that its impedance at the working frequency was of a capacitive nature, with an equivalent capacitance of 67 pF. At a coil inductance of 1.1 μH the additional parallel capacitance was around 60 pF, which made it possible to connect a variable capacitor with a working point shifted to the region of optimum steepness of the characteristic. This, in turn, provided reliable operation of a tight phase-locking system[13] for automatic fine tuning of the natural frequency of the LC circuit. By decreasing the phase shift between the voltage of the power oscillator and the voltage across the circuit by a factor of about five, the phase-locking system permitted a 25–30-fold reduction in the influence of the frequency characteristic and vibrations of the circuit on the size of the output signal of the Q meter.

The NMR spectra, which consisted of a periodic sequence of signals 5 msec long with a repetition frequency of 50 Hz, were continuously observed on an oscilloscope (see Fig. 1) and also fed to an analog integrator whose output was sent to a digital voltmeter and a chart recorder. A preliminary processing of the spectra was done with CAMAC-standard apparatus. After passing through a KA209 analog-digital converter[14] and a KL006 buffer memory[15] the spectrum, converted into digital form, was stored in the memory of a KM-001 microcomputer.[16] The preliminary processing provided for: storage and averaging of the spectra for the purpose of extracting the signal from the noise and interference (we ordinarily used an accumulation of up to 400); integration; output of the spectrum to graphic display; and writing to the magnetic tape of an RK-1 cassette memory.

The final processing of the DMR spectra was done on a BÉSM-6 computer and consisted of three main steps.

1. Conversion of the mass of data to a linear frequency scale. This conversion made use of the correponding characteristic of the power oscillator in the form of the dependence of the frequency on the time interval from the start of the sweep.

2. Evaluation of the deuterium polarization P_D by relation (4). Under the assumption that the electric-field-gradient tensor of the diol molecules is axially symmetric,[17] the function F describing the total DMR spectrum can be written as a superposition of two curves, φ and φ_a, which are symmetric with respect to ν_D (see Fig. 1):

$$F=\varphi+R\varphi_a \quad (R>1). \tag{5}$$

To this we add the most general assumptions[6]: $\varphi_a' < 0$ in the region $(\nu_D - 3\nu_Q, \nu_D + 6\nu_Q)$ and $\varphi' > 0$ in the region $(\nu_D - 6\nu_Q, \nu_D + 3\nu_Q)$.

Suppose F is expanded in a Fourier series with coefficients A_n and B_n, i.e., $F\sim(A_n, B_n)$. For the functions φ and φ_a we have $\varphi_a \sim (a_n, b_n)$, $\varphi_a \sim (a_n, -b_n)$; then

$$A_n=a_n(1+R), \quad B_n=b_n(1-R). \tag{6}$$

The value of R is sought by the method of successive approximations. Using the value R_i (i is the number of the iteration) and formulas (6), we find a_n^i and b_n^i and then sum the corresponding series to obtain the functions Ψ_i and Ψ_{ai}, which are shown by curves 2′ and 3′ in Fig. 1. The oscillatory parts of these functions are then replaced by second-degree or higher polynomials which satisfy the condition of monotonicity. The newly obtained functions φ_i and φ_{ai} are shown by curves 2 and 3 in Fig. 1. If R_i is sufficiently close to R we should have

$$\delta \equiv \left| \int_{\nu_D-6\nu_Q}^{\nu_D+6\nu_Q} (\psi_i - \varphi_i)\, d\nu \right| \leqslant \varepsilon, \tag{7}$$

where ε is the specified measure of accuracy of the calculations; usually $\varepsilon \approx 10^{-3}$. If inequality (7) is not satisfied, then δ is used to determine R_{i+1} for the $(i+1)$th iteration.

3. The calculated values of the polarization should be corrected for the systematic errors of the Q meter.[13] These errors were calculated for the experimentally observed absorption line shape by the programs described in Ref. 13. It was found that P_{meas}—the polarization determined from the asymmetry of the spectrum obtained with our Q meter—should be corrected by the formula

$$P_D=P_{\text{meas}}(1\pm0.06),$$

where the plus sign is for a positive polarization and the minus sign for a negative polarization. As in Ref. 9, we made sure that for all of our recorded DMR spectra the ratio of the sum of the shape functions of the spectrum at the peaks to the integrated intensity of the spectrum remained constant to within 1% or better. This was used as one of the reliability criteria for the recorded information.

RESULTS AND DISCUSSION

The main results are given in Table I. The listed values of the polarization were obtained after 2–2.5 h of continuous pumping at the optimum conditions in terms of both the frequency and the microwave power level. During the pumping the total power dissipated in the dissolution chamber was 10 mW, a value which gives about 1 mW/g for the specific microwave power arriving at the sample. The optimum frequency was determined from the experimental data which are shown in Fig. 3 in the form of a plot of the maximum attainable polarization versus the microwave frequency for samples No. 1 and No. 3. The difference between the frequencies corresponding to the peaks for the positive and negative polarizations is 230 MHz. Between these two peaks there are no other noticeable peaks as might correspond, for example, to the differential solid effect.[8] This suggests that the main contribution to the deuteron polarization is from the dynamic cooling effect. To confirm this hypothesis we did several experiments similar to those described in Ref. 8. After the maximum deuteron polarization is reached, the pumping is turned off and the apparatus is readjusted for observation of the proton magnetic resonance (PMR) signal, which, in accordance with the single spin temperature, has also reached its maximum value. In addition, we used the

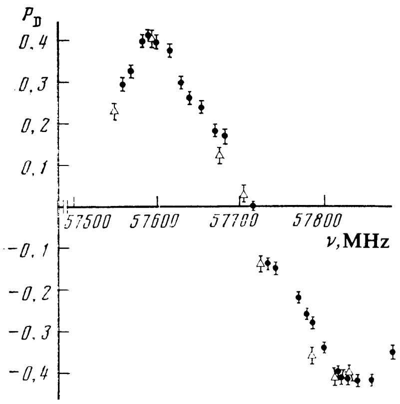

FIG. 3. Maximum attainable deuteron polarization versus the frequency of the microwave field: (●) for ethanediol, (△) for propanediol-1,2.

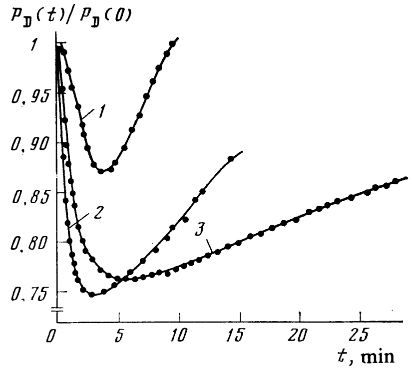

FIG. 4. Changes in the deuteron polarization (spin temperature) after the microwave pump is turned on at unequal temperatures of the proton and deuteron spin systems: curve 1 was obtained for a microwave power one-and-one-half times as large as for curves 2 and 3; curve 2 is for a negative polarization (spin temperature), curves 1 and 3 for a positive polarization.

saturation of the PMR line: an rf voltage fed to the induction coil at a frequency equal to the central frequency of the spectrum caused a decrease in the proton polarization (or, equivalently, a "heating" of the proton NSS) by a factor of two or three. Then we again observed the DMR signal, which, of course, was unchanged, since without pumping and in a high field there is virtually no contact between the spin systems. We then resumed pumping and observed the changes in the polarization (or of the spin temperature) in the deuteron NSS (Fig. 4). Immediately after the microwave pump was turned on ($t = 0$) we observed a growth of the spin temperature (a decrease in the polarization) in the deuteron NSS and a simultaneous drop in the spin temperature in the proton NSS (not shown in Fig. 4), so that within 5–10 min after the minima on the curves the spin temperatures of all the spin systems have equilibrated. After this there is a common lowering of the spin temperature under pumping. The three curves in Fig. 4 were obtained at different microwave power levels; as one would expect, at high power the time required to establish a single spin temperature is shorter and the relative drop in the NMR signal is smaller. This effect—the appearance of an induced contact among all the NSS when the material was irradiated by a microwave field—was observed for all three samples listed in Table I. The line of the EPR spectrum recorded for sample No. 1 at a temperature of 0.3 K has an approximately bell-shaped form with a half-width about equal to the difference between the pumping frequencies corresponding to the maximum positive and negative polarizations: 230 MHz or 82 G. Thus our entire set of data confirms the hypothesis that the main mechanism responsible for the dynamic polarization of deuterium in our samples is dynamic cooling.

Sample No. 2 also had no differential-solid effect, and the maximum values of the polarization of both signs were reached at the same frequencies as for sample No. 1. Thus the change in concentration did not affect the ERP linewidth at 0.3 K. The fact that the EPR linewidth is independent of the concentration of paramagnetic centers indicates that the main cause of the broadening is anisotropy of the electron g factor. For this reason one expects that increasing the magnetic field to 3 T will lead to only an unimportant increase in the deuterium polarization, and a further increase in the magnetic field will not increase the maximum polarization.[8]

The relaxation time τ_1 given in Table I was obtained from measurements in a magnetic field of 0.32 T under the assumption of an exponential decay of the polarization: $P = P_0 e^{-t/\tau_1}$. Extrapolation of these data to temperatures around 20 mK (Ref. 8) at the same magnetic field gives $\tau_1 \geqslant 100$ h, a value which is quite sufficient for using these materials in frozen polarized targets.

CONCLUSION

1. We have obtained a polarization of ± 0.40 for deuterium nuclei in a material consisting of a Cr(V) complex in completely deuterated ethanediol and propanediol-1,2 (see Table I).

2. Our studies have established that the main mechanism for the dynamic polarization of nuclei is the dynamic cooling effect. Our data also suggest that an external magnetic field with an induction from 2 to 3 T is optimum for obtaining the greatest nuclear polarization.

3. The measured values of the relaxation time of the nuclear magnetization in a weak field indicate that the investigated materials should be suitable for use in frozen polarized targets.

We wish to thank Yu. M. Kazarinov and S. B. Nurshev for support of the experiments and B. S. Neganov and Yu. F. Kiselev for helpful discussions. We are grateful to L. P. Meshchanin, V. P. Dan'shin, O. N. Shchevelev, and A. F. Prudkoglyad for assistance in running the experiments. We take this opportunity to express our appreciation to N. N. Zatsepina and I. F. Tupitsin for developing and implementing the technique for obtaining deuterated diols, and to A. P. Yur'eva and N. N. Bubnov for assistance in analyzing the samples.

---

[1] B. S. Neganov, Vestn. Akad. Nauk SSSR **12**, 49 (1968); B. S. Neganov, Proc. Internat. Conf. on Electromagnetic Interactions at Low and Medium Energies, Dubna, 1967, publ. Vol. 4 [in Russian], Moscow (1967), p. 303.

[2] D. Hill, R. C. Miller, M. Krumpolc, and S. Roucek, Nucl. Instrum. Methods **150**, 331 (1978).

[3] S. Hiramatsu, S. Isagawa, S. Ishimoto, A. Masaike, and K. Morimoto, in: High Energy Spin Physics, 1982, AIP, New York (1983), p. 512.

[4] É. I. Bunyatova, R. M. Galimov, S. A. Luchkina, Preprint OIYaI 12-82-732, Joint Institute for Nuclear Research, Dubna (1982).

[5] É. I. Bunyatova and N. N. Bubnov, Preprint OIYaI D-1-82-805, Joint Institute for Nuclear Research, Dubna (1982); Nucl. Instrum. Methods **219**, 297 (1984).

[6] A. Abragam, The Principles of Nuclear Magnetism, Clarendon Press, Oxford (1961).

[7] M. Goldman, Spin Temperature and Nuclear Magnetic Resonance in Solids, Clarendon Press, Oxford (1970).

[8] W. De Boer, Preprint CERN 74-11, Geneva (1974).

[9] N. S. Borisov, É. I. Bunyatova, A. G. Volodin, et al., Preprint OIYaI 1-80-98, Joint Institute for Nuclear Research, Dubna (1980).

[10] N. S. Borisov, É. I. Bunyatova, and Yu. F. Kiselev, Proc. Internat. Symp. on Polarization Phenomena in High-Energy Physics [in Russian], D 1, 2-82-27 Dubna (1982).

[11] V. A. Atsarkin, Dinamicheskaya Polyarizatsiya Yader v Tverdykh Diélektrikakh, (Dynamic Polarization of Nuclei in Solid Dielectrics) Nauka, Moscow (1980).

[12] C. D. Jeffries, Dynamic Nuclear Orientation, Interscience, New York (1963).

[13] M. Yu. Liburg and V. N. Matafonov, Preprint OIYaI R-13-81-365, Joint Institute for Nuclear Research, Dubna (1981).

[14] F. Gabriel', A. I. Kalinin, S. I. Merzlyakov, E. Richter, E. Tissold, and W. Fromm, Preprint OIYaI R-13-11201, Joint Institute for Nuclear Research, Dubna (1978).

[15] V. A. Antyukhov, Dao Vi Vyong, Z. Dinal, et. al., Preprint OIYaI 10-80-650, Joint Institute for Nuclear Research, Dubna (1980).

[16] V. T. Sidorov, A. N. Sinaev, and I. N. Churin, Preprint OIYaI R-10-12481, Joint Institute for Nuclear Research, Dubna (1979).

[17] O. Hamada, S. Hiramatsu, S. Isagawa, S. Ishimoto, A. Masaike, and K. Morimoto, Nucl. Instrum. Methods **189**, 561 (1981).

Translated by Steve Torstveit